AIAA-98-2539

EFFICIENT VISCOUS DESIGN OF REALISTIC AIRCRAFT CONFIGURATIONS

Richard L. Campbell*
NASA Langley Research Center
Hampton, VA

Abstract

This paper addresses the use of the Constrained Direct Iterative Surface Curvature (CDISC) design method in the aircraft design process. A discussion of some of the requirements for practical use of CFD in the design process is followed by a description of different CFD design methods, along with their relative strengths and weaknesses. A detailed description of the CDISC design method highlights some of the aspects of the method that provide computational efficiency and portability, as well as the flow and geometry constraint capabilities. In addition, an efficient approach to multipoint design, the Weighted Averaging of Geometries (WAG) method, is described and illustrated using a couple of simple examples. The CDISC and WAG methods are then applied to a complex generic business jet geometry using an unstructured grid flow solver to demonstrate the multipoint and multicomponent design capabilities of these methods.

Introduction

During the last two decades, computational fluid dynamics (CFD) has become an integral, perhaps even dominant, part of the aircraft aerodynamic design process[1,2]. The confidence in and reliance on computational methods has increased for a variety of reasons. First and foremost, improvements to computer hardware and flow solver algorithms have significantly reduced the time required for flow analysis. For example, the use of convergence acceleration techniques such as multigrid, along with multitasking on supercomputers and/or parallel machines, has made it possible to perform Navier-Stokes analysis on dense viscous grids around complex configurations in a day or two. Another important factor contributing to increased CFD usage has been the improvement in grid generation methods. In particular, the use of overset, unstructured and Cartesian grids have reduced the time required to develop grids around nearly complete aircraft configurations from months to days in many cases. A third reason for increased use of CFD in the design process is the improved accuracy achieved from the use of Navier-Stokes codes with new turbulence models. While coupled inviscid/boundary-layer methods are still adequate at cruise and other conditions where the flow is primarily attached, Navier-Stokes codes are needed for the more demanding flight conditions such as buffet onset, and the one- and two-equation turbulence models have produced good correlations with experimental data in some cases.

Even though CFD has produced some results that rival the accuracy of wind tunnel data, it has not replaced the wind tunnel and is not likely to do so in the near future. In spite of the improvements in computational speed, the wind tunnel is still a much more effective means of acquiring the large volume of data needed to evaluate a configuration across the flight envelope. The wind tunnel is also used to obtain data at the edges of the flight envelope where considerable flow separation is present. Although improvements have been made, CFD is still not consistently accurate enough to be the sole source of data at these flow conditions.

While CFD has not replaced the wind tunnel, it has been elevated to a partner status in the design process because of the improvements listed above and also because of the unique contributions that it makes that cannot easily be duplicated in a wind tunnel. Although CFD solutions are typically only obtained for a few conditions, this still allows a fairly rapid evaluation of new configurations at key conditions such as cruise. Also, each computation produces a wealth of flow field data that cannot practically be obtained in type or quantity in the wind tunnel. This makes CFD invaluable

*Senior Research Engineer, Senior Member of AIAA

Copyright @ 1998 by the American Institute of Aeronautics and Astronautics, Inc. No copyright is asserted in the United States under Title 17, U. S. Code. The U.S. Government has a royalty-free license to exercise all rights under the copyright claimed herein for Government purposes. All other rights are reserved by the copyright owner.

in locating and diagnosing problem areas that lead to poor aerodynamic performance. This capability also points to what may be the most important advantage that CFD has over the wind tunnel - the ability to rapidly develop configurations that have improved aerodynamic performance. While expert aerodynamicists in the past certainly did produce configurations with good performance using cut-and-try approaches in the wind tunnel, the automated CFD design methods available today can produce significantly improved configurations in much less time. This is not to say that expert aerodynamicists are no longer needed, but that they now have additional tools to help them achieve their goals. These goals include not only producing a design with the best performance, but also reducing the time required to do so. This will be accomplished both by reducing the time to complete each design cycle as well as by reducing the number of cycles needed to arrive at the final configuration.

The author had the opportunity to observe the impact of CFD in the aircraft design process first-hand in 1996 when he and other NASA personnel were invited to participate on-site in the design of the MD-XX commercial transport at what was then the Douglas Aircraft Company (DAC). This cooperative effort had a two-fold objective: 1) to assist DAC in the application of CFD analysis and design methods developed by NASA; and 2) to expose the developers of these methods to the actual design environment so that future codes might be more readily adapted into the design process. While the airplane project was eventually cancelled, the CFD codes were successfully used to produce a configuration with good aerodynamic performance, and participation in the process yielded some insights into the strengths and weaknesses of the CFD methods. These insights, along with information gathered from discussions with designers and aerodynamicists from other companies, led to the following list of desirable attributes in a CFD analysis or design method that is to be used in a design project environment: quick set-up time, robustness, short turnaround time, accuracy, and ease in interpreting the results. For design methods, the capability of including geometry as well as flow constraints were also important features. Since this list is fairly generic, some specific comments on each item, particularly as it relates to design codes, will be given below.

Surface definition and grid generation are still the big drivers in determining the setup time for a design, especially for complex configurations. While multiblock grids have been generated around configurations with multiple components, the process is tedious, especially if point-matching at the block interfaces is required. Overset structured grids are easier to develop and were used extensively in the MD-XX project, but even they can present problems in juncture regions. The most promising approaches to quick grid generation for complex configurations appear to be the unstructured and Cartesian grid methods, where grid generation times are measured in days as opposed to weeks or months. It should be pointed out, however, that most design methods use grid perturbation methods, so that the ease of modifying a grid becomes more important than the initial grid generation time. The set-up time for a design problem is also affected by the selection of design variables, constraints, etc., but as experience in using the various methods is gained, this appears to be less of an issue. Code robustness is also an important factor in reducing design cycle time. This often has to be traded against the desire for shorter turnaround times since acceleration techniques such as multigrid or larger time steps occasionally lead to less stability in the flow solver. From the author's experience, it is best to specify flow solver convergence levels between design cycles and the size of design changes to ensure a successful code run even at the expense of speed, since submitting a second run after a code failure generally takes longer than a slower first run.

One important issue that became apparent during the MD-XX design experience was the requirement for accuracy in the design process. Accuracy is affected by factors such as geometric complexity and fidelity, grid resolution, and modeling of the flow physics. For this configuration, some designs were performed where these factors were lacking and the projected benefits were not realized when the new configuration was analyzed in the primary code used for drag evaluation. This result made it clear that, while simpler configurations and grids may be useful for preliminary studies, a design method that uses the same grids and flow solver that is used for final analysis would be highly desirable.

A final observation relates to the need to include both flow and geometry constraints in the design process. Unconstrained designs can give an indication of ultimate potential improvements, but requirements from other disciplines such as manufacturing and structures will limit what can actually be obtained. Even within the aerodynamic discipline, requirements from other design conditions can restrict the benefit that can be achieved at a primary design point. This points to the need for a constrained multipoint design capability that can include these influences early in the design process. It also became apparent during the MD-XX design exercise that a tool that would allow the designer to quickly assess how well a design met these constraints

and design objectives would be very useful. In general, this was accomplished through various plotting packages, but the process was not very efficient. With these observations in mind, the following section will discuss some of the types of automated CFD design methods that are currently available, their relative strengths and weaknesses, and how they can complement one another in the design process.

Design Methods

In the aerodynamic design process, the following three questions must be addressed: 1) what is the desired flow improvement?; 2) how can that improvement be obtained?; and 3) what factors tend to limit the improvement? The first question usually relates to a global aerodynamic parameter such as lift or drag that is, in turn, tied to a global aircraft parameter such as range or fuel efficiency. This parameter is ultimately related to customer mission and/or cost requirements.

The question of how to obtain the desired improvement in the global aerodynamic parameter can be approached in a couple of ways. The parameter can be directly addressed in the formulation of an objective function for optimization (e.g., minimize drag). This approach has the advantage of not requiring any a priori knowledge of relationships between geometry and flow changes, but tends to be expensive since this information must be determined computationally. Often, however, the desired flow improvement is indirectly obtained by relating it to another flow characteristic. For example, induced drag may be reduced (at least in theory) if the spanwise loading is moved toward an elliptic distribution. Similarly, wave and viscous drag components can be reduced by specifying chordwise pressure distributions that have reduced shock strengths and mild pressure gradients, respectively. This indirect approach requires that the designer have a good understanding of the physics that underlie the flow improvement, but may allow designs to be obtained at less expense if the relationships between geometry changes and these flow parameters are known.

In order to answer the second question, then, the designer must determine: a) what gets changed to try to bring about the improved flow; and b) what are the magnitude and direction of those changes. The first part involves the selection of design stations and design variables and, depending on the design method, can play an important role in determining the ultimate cost of a design. The main factor in the cost of a design, however, is tied to how b) is answered; i.e., what design method will be used to determine the changes. A number of methods are available, each with its own set of advantages and disadvantages that the designer must consider, all within the context of computer resource and time limitations. Some of the types of methods are discussed below, generally in order of decreasing time required.

The first category of design method considered is general search methods, such as genetic algorithms[3,4] and simulated annealing methods[5]. These methods have been receiving more attention recently because of their ability to search a design space that has multiple minimums. The methods are also very robust since only the value of the objective function, and not its gradient with respect to the design variables, is required. The major disadvantage of these methods is that they typically require hundreds or thousands of analysis runs to evaluate the design space for even fairly simple cases. Also, these methods do not try to locate the actual minimum, so that once the region of the minimum is found, a gradient-based method must then be used to search for the final minimum value.

Probably the most widely used design methods fall into the category of gradient-based optimization. This process involves computing the sensitivity derivatives of the objective function with respect to the design variables, estimating the design changes that will lead to improvement, then making the changes and reevaluating the new design. The simplest but most costly method for determining the sensitivity derivatives is the finite-difference approach[6-8]. This method typically requires hundreds of analysis runs for a single 3-D design case. One approach that reduces the time required to obtain the derivatives, although at the expense of increased computer memory, is to compute the derivatives analytically. In some cases[9], the derivatives are already available as part of the flow analysis method, but in general additional code must be generated to differentiate the flow equations. This coding can be manually generated[10] or may be developed using an automated method such as ADIFOR[11]. In reference 11, the differentiation has been implemented in an incremental iterative form that significantly reduces the high memory requirements usually associated with sensitivity analysis. Another approach that appears to be even more efficient is the adjoint method[12-15]. Like the analytic approach just described, this method also requires additional coding to solve one or more flow adjoint equations, but the additional memory requirements are nominal, and this approach can reduce the cost of determining the sensitivity derivatives for each design cycle to about twice the cost of a flow solution. This approach has been implemented with both Euler and Navier-Stokes flow solvers and the time for a design is reported to be about 20-50 equivalent analysis

runs. Both the automated differentiation and adjoint approaches are closely tied to specific flow solvers and are thus not easily coupled with other codes. The finite-difference approach, in contrast, is very portable.

As discussed above, an advantage of the general search methods as well as the gradient-based methods is that they do not require an understanding of the flow physics that relate to an improved design. Thus they can actually be used to determine what flow state will lead to improved aerodynamic performance. This information, whether obtained from optimization, analytical studies, or empirical data, is a crucial requirement for the third category of design codes, knowledge-based methods. These methods are usually much faster than the above approaches because the sensitivity derivatives are already known, at least approximately, so that the only time involved is for the iterative application of the design rules to determine a final configuration. Like the finite-difference optimization approaches, these methods tend to be modular and easily coupled with different flow solvers. The Constrained Direct Iterative Surface Curvature (CDISC) design method[16-18] falls into this category and will be described in the subsequent section.

The third design question, that of what limits the design, is usually expressed in terms of flow and geometry constraints. Geometry constraints, such as thickness or leading-edge radius, are generally easy and inexpensive to incorporate into a design method since they do not require information from the flow solver. The only issue that can arise with some methods is compatibility with target pressure distributions. This difficulty can usually be avoided by not specifying the entire pressure distribution, but by prescribing only characteristics such as gradients or maximum levels in regions of importance. Flow constraints, such as lift or pitching moment, can be more costly to use, especially for the adjoint method which requires separate adjoint equations to be programmed and solved for each flow constraint (unless it can be expressed as a penalty to the objective function). Also, the performance of the configuration at off-design conditions can be used as a flow constraint, which adds at least one additional flow solution per design cycle regardless of the design method.

CDISC Design System

A flow chart for the CDISC design system is shown in figure 1. The CDISC module (shown in gray), is indirectly coupled with a flow solver using a Unix script. After a user-specified number of flow solver iterations, the current geometry and flow variables are sent to the CDISC module via grid and restart or flow solution (such as PLOT3D) files. The surface coordinates and pressure coefficients at the design stations are then extracted. For structured grids, this extraction is done within the CDISC module. For unstructured grids, it was necessary to develop auxiliary codes to perform this function as well as to interpolate the design changes back to the grid points[19]. These auxiliary codes have recently been extended to allow design stations to be defined along geometric patch boundaries in addition to the original arbitrary cutting planes.

Once the required surface information is obtained, the target pressure distributions needed in the basic DISC module are developed by systematically modifying the current analysis pressures based on the flow constraints. As an alternative, a prescribed target pressure distribution can be input, but experience has shown that this approach is usually less robust and slower to converge, since knowing in detail what the pressures should be at every point on the surface is difficult. The constraint approach tends to modify only pressures in selected regions to achieve the desired characteristics, allowing the flow in other areas to develop as required to maintain a reasonable geometry.

The flow constraints in CDISC can be grouped into 3 general categories: 1) global, which influence multiple design stations (e.g., spanload distribution); 2) section, which affect values on both surfaces of an airfoil (section lift or pitching-moment coefficient); and 3) surface, which are applied to a single aerodynamic surface (shock strength or pressure gradient). Multiple passes are made through the flow constraints in an attempt to satisfy all of the requirements. Since the constraints can be prioritized, optimization can be simulated by overconstraining a given value and letting the CDISC module adjust it to the minimum value that will allow the higher-priority constraints to be satisfied.

An example of a flow constraint that combines both section and surface characteristics is illustrated in figure 2. This constraint modifies the baseline target pressures to define an “optimum” supercritical rooftop pressure distribution for a given lift coefficient. To accomplish this, an empirically-derived expression for the maximum allowable supercritical compression gradient is adjusted in level, with the aft extent determined from another expression for reasonable shock location, until the desired lift coefficient is obtained. For the design result shown, the pitching moment was also constrained to match that of the original airfoil, resulting in changes to the pressures in other regions as well. The point of this example is that the flow constraints in CDISC were

able to automatically produce a target pressure distribution that met the lift and moment requirements while reducing the drag coefficient from 0.0166 to 0.0100. It should be noted that, since the empirically-derived expressions for the rooftop are related to the surface geometry, the target was redefined for each design cycle based on the current flow and geometry characteristics.

The CDISC module then uses the basic DISC method[20] to modify the surface geometry to match the target pressures. This method was originally based on analytically-derived expressions relating a change in surface curvature to a change in surface pressure coefficient. Recent studies have indicated that functions based on Mach number give better results than the original pressure functions; therefore these new Mach-geometry relationships have been used for the results shown in this paper. Since these relationships (one for subsonic local flow, one for supersonic) are known ahead of time, and the design can be converged in parallel with the flow solution, the DISC approach is a very efficient way of solving this inverse problem. The method can be used at subsonic, transonic, or supersonic speeds and, although strictly valid only for attached flows, it has been successfully used for design at buffet-onset conditions when significant flow separation was present.

The new design surface geometry is evaluated relative to the geometry constraints and, if violations are found, it is further modified to meet those constraints. In this sense, geometry constraints take precedence over flow constraints, although in most cases both sets of constraints are met by the final design. As with the flow constraints, global, section, and surface geometry constraints may be specified and multiple passes are made through the constraints in an attempt to satisfy all of them. Some of the geometry constraint options that are available include twist distribution, local or maximum thickness, leading-edge radius, trailing-edge included angle, volume, chordwise and spanwise curvature, and a hard surface. The hard surface constraint is used to define a region that the design surface is not allowed to enter and will be illustrated in a later design example.

The final operation required before returning to the flow solver is to modify the computational grid to reflect the new surface geometry. For structured grids, the changes in surface geometry are linearly lofted along grid lines between design stations. The volume grids are then perturbed to reflect the surface changes either within the CDISC module, or by using some auxiliary grid projection tools developed for use with overset grids[21]. For unstructured grids, the design changes are linearly interpolated to the surface grid points, and the volume grid is modified using the spring analogy[19].

The new volume grid is then returned to the flow solver and the solution is continued using the old restart file. Since the old flow variables are assigned to points which may have changed locations, a spike in the residual typically occurs, but the level usually drops quickly and by the final design cycle has returned to a reasonable level of convergence. Since the flow solver does not have to be fully converged after each design cycle, it is usually possible to obtain a well-converged design in 10-20 design cycles, which takes approximately as much time as a single converged flow analysis. While a minor time penalty due to multiple restarts is incurred with this indirect coupling approach as compared to a direct coupling of CDISC with the flow solver, it yields benefits such as ease of portability and code maintenance as well as reduced flow solver memory requirements. The CDISC module has been indirectly coupled with several block-structured grid Navier-Stokes flow solvers (TLNS3DMB[22], CFL3D[23], PAB3D[24], and FLOMG[25]), the OVERFLOW overset-grid flow solver[26], and with the USM3D[27,28] and FUN2D[29] unstructured-grid flow solvers.

Multipoint Design with CDISC

As mentioned earlier, it is highly desirable for an aerodynamic design method to account for requirements imposed by other disciplines as well as other flow conditions. While the CDISC method described in the previous section does allow for disciplines such as structures and manufacturing to influence the design through the geometry constraints, it does not generate sensitivity information that could be used in a multipoint optimization method. In order to provide a multipoint design capability that is consistent with the goal of using the same grids and flow solver that are used for final analysis, the following simple procedure, referred to as the Weighted Averaging of Geometries (WAG) method, was developed.

A flow chart illustrating the WAG method for a two-point design problem is shown in figure 3. In this procedure, geometries developed from designs at each of the design points will be used as shape functions and combined to minimize an objective function. The process begins by performing a design at each of the design points, then analyzing the resulting geometries at the other design conditions. An objective function is formulated based on the drag coefficients at each design condition, and the function is evaluated for each of the two configurations. For example, if the two design

points were of equal importance, the objective function for a given configuration would simply be the average of the drag coefficients at the two conditions. At this point, the objective function is known for the two configurations and would indicate which of the two is better for the mission, but there is no information about how to combine the two geometries. A random guess of a geometry weighting factor could be made, but a more accurate estimate can be obtained by assuming a quadratic variation of drag with geometry weighting factor, then computing the value of weighting factor that yields the minimum value of the objective function. The WAG method automatically combines the two geometries using this weighting factor to produce a new surface geometry. The new surface definition is fed into CDISC, which then modifies the volume grid for one of the configurations. This blended configuration is then analyzed at both design conditions, and a new geometry weighting factor is computed. In determining the new factor, the assumption of a quadratic variation of drag with weighting factor is no longer used; instead, a curve-fit procedure is used to estimate a new minimum for the objective function. Convergence is obtained when the new minimum is within a specified tolerance of the previous minimum (typically .02 in weighting factor).

To illustrate the WAG approach, an airfoil has been designed at start-cruise and end-cruise conditions using the FLOMG code. The results are shown in figure 4, where a weighting factor of 0.0 represents the end-cruise design geometry and a weighting factor of 1.0 represents the start-cruise geometry. The dashed lines show the assumed quadratic variation of drag away from each design point, and the solid line shows the resulting variation in objective function, which for this case was a 50/50 combination of the drag at the two design conditions. The initial estimate had the minimum objective function occurring at a weighting factor of 0.48, so the start- and end-cruise geometries were blended using this factor and the new configuration was analyzed. The resulting drag values at the start- and end-cruise conditions are plotted as a square and triangle, respectively, and indicate that the quadratic estimates were reasonable. The plus sign is the new computed objective function and falls very close to the estimated curve. A new minimum was computed using the additional data and the curve fit procedure, but since it yielded the same weighting factor, no additional multipoint cycles were needed. The combined drag objective function for the multipoint design was reduced by about 2 drag counts over the best of the single point designs.

Because this is such a simple approach, the question arises as to how it would compare with formal multipoint optimization. As part of a cooperative program with what was then the Defense Research Agency (DRA), CDISC-WAG and numerical optimization were both applied to the dual-point design of a generic fighter wing/body configuration[30]. The surface grid used for the TLNS3D/CDISC Euler computations is shown in figure 5. The two design points were $M=0.9/C_L=0.45$ and $M=1.6/C_L=0.125$, which represented mild maneuver conditions at each point. The design was performed on the wing only and thickness, camber, and twist changes were allowed, subject to lift and maximum thickness constraints. Dual-point designs were performed for a range of missions that varied the weighting on the drag factors from an all-transonic mission to an all-supersonic one.

The results from the two design approaches are shown in figure 6, where the drag at each point is normalized based on the drag of the baseline configuration at those conditions, computed by the flow solver used by each design method. This normalization was done in an attempt to remove discrepancies resulting from the use of different grids and flow solvers. The left end of the curve represents a design for an all-transonic mission, with low transonic drag (C_{Dtr}) and high-supersonic drag (C_{Dss}). It can be seen that the two design approaches gave similar results, with CDISC-WAG doing a little better for missions weighted more toward the supersonic design point and the formal multipoint optimization having a slight advantage for transonic missions. The cost of generating the designs was considerably different, however, with the numerical optimization procedure requiring several hundred flow analyses per mission design, whereas CDISC-WAG required the equivalent of 8 flow analyses for the first mission design, and generally only two more analyses for each additional mission.

Design Applications for Complex Configurations

While the design examples shown so far have illustrated the effectiveness and efficiency of the CDISC and WAG design approaches, they have used simple geometries where the designs could have been accomplished in a reasonable amount of time using optimization. CDISC has been applied to a number of complex configurations using large Navier-Stokes grids as part of either NASA focused programs or company in-house projects. While specific results from these design activities are either limited in distribution or proprietary, some general comments on the performance of CDISC can be made.

As mentioned before, CDISC combined with the OVERFLOW code was used in the design of the MD-XX commercial transport. The designs were performed on wing/body/nacelle grids having over 5 million grid points and required only about 70 percent as much time as the original converged analysis run. The final design reduced the drag at cruise by several counts relative to the baseline wing (which already had good performance), and maintained good off-design characteristics. This CDISC/OVERFLOW system with large viscous grids has also been used by Boeing-Long Beach personnel to work on nacelle integration issues for a Blended Wing Body advanced transport configuration. Significant reductions in wave drag have been obtained and flow separation issues associated with propulsion/airframe integration are currently being addressed. Finally, CDISC with OVERFLOW was applied to a supersonic transport configuration that had already been optimized using a full-potential design method. The OVERFLOW grid had over 13 million grid points and modeled the fuselage, wing, nacelle, and diverters as viscous surfaces. At the supersonic cruise point, CDISC was able to redesign the wing to achieve additional drag reduction, probably because using the Navier-Stokes code allowed the design to be done with the nacelle/diverter shock system accurately modeled. Design at the supersonic cruise point took slightly longer than a converged analysis run, while designs at the transonic cruise point required less time than a flow analysis at that same condition.

Design of a Generic Business Jet

To demonstrate the application of the CDISC and WAG design methods to complex configurations, a generic business jet geometry was chosen. This configuration was supplied to NASA by Cessna personnel for the purpose of demonstrating grid generation capabilities and was not necessarily intended to have good aerodynamic performance. The geometry definition included a fuselage, wing, wing fairing, pylon, and flow-through nacelle. The USM3D flow solver was chosen for the design, and an unstructured inviscid grid having about 780,000 cells was generated using the VGRID grid generation code[31]. A viscous unstructured grid having about 1.3 million cells was also generated, but a problem in the USM3D viscous flow solver precluded its use in this exercise. Since viscous effects are very important for correctly modeling the flow over supercritical wings at transonic speeds, the interacted boundary layer (IBL) capability was used. The Euler/IBL approach requires significantly less time and memory than Navier-Stokes computations and would probably be the preferred method for developing the initial configuration anyway, with subsequent Navier-Stokes analysis and re-design done if needed.

The surface grid for the generic business jet is shown in figure 7 (the grid has been mirrored across the symmetry plane to show the whole configuration). The objective of the following designs was to reduce the cruise drag of the aircraft while maintaining various flow and geometry constraints. No design conditions were supplied with the generic business jet geometry, so two cruise design points were selected based in the leading-edge sweep of 15 degrees and airfoil thickness-to-chord ratios ranging from about 0.15 at the root to 0.10 at the tip. The primary design point was M=0.75/ C_L=0.48 and the secondary design point was M=0.78/ C_L=0.42.

The usual design approach with CDISC is to obtain an initial analysis of the baseline configuration, then evaluate the potential for reducing the induced, wave, and viscous drag components. A solution was obtained for the baseline configuration at the primary design point, converging about 3 orders of magnitude and requiring about 2.6 hours of CPU time and about 140 MW of memory on a Cray C-90. The resulting local Mach number contours are shown in figure 8. A moderate shock can be seen on the wing, with strong shocks present on top of the fuselage just aft of the canopy and on the aft fuselage in the vicinity of the pylon and nacelle. This would imply that reductions in wave drag could probably be obtained. An examination of the spanload indicated that it was already close to elliptical and that there was little room for improvement in the induced drag. While the Euler/IBL method would not allow direct evaluation of viscous drag problems due to separation, the issue was addressed indirectly by designing for weak shocks and mild recovery gradients on the wing and ensuring that shocks on other components were reduced below M=1.3 to avoid shock-induced separation.

Single-Point Wing Designs

The first design exercise attempted to reduce the wing drag at the primary design point by using the optimum rooftop constraint shown earlier, along with other constraints to maintain the section lift and pitching-moment coefficients of the baseline wing. In addition to these flow constraints, geometry constraints were imposed to retain the original maximum thickness and thickness at two spar locations (x/c=0.3 and 0.7), along with a leading-edge radius that is at least 90 percent of the original value. In addition, a manufacturing constraint that the wing thickness be at least 10 percent of the distance from the trailing edge (e.g., the wing must be at least one inch thick at a

location ten inches ahead of the trailing edge) was enforced from the trailing edge forward to the rear spar. The CDISC method was run for 20 design cycles and required about 2.0 hours. The resulting pressure distributions and airfoils at semispan locations of 0.4 and 0.8 are shown in figure 9. The design pressures match the rooftop targets very well and have reduced shock strengths and recovery gradients at both stations. These results were obtained with very minor changes to the airfoil sections and all of the constraints were met.

The convergence history for the initial baseline analysis and subsequent wing design is shown in figure 10. The sharp spike in the residual at 50 iterations marks the beginning of the boundary layer interaction, followed by steady convergence to the required level at 300 iterations. At this point, the design was initiated, and all three parameters in the figure change significantly. By the end of the design, however, the minimum residual has returned to its former level and the desired lift level has been recovered. The drag, though still showing some small oscillations, indicates a reduction of about 11 counts relative to the baseline. Note that all drag values given in this paper have been corrected to account for small variations in lift between the designs and the original baseline.

The same set of flow and geometry constraints was then applied to the wing at the secondary design point of M=0.78 and C_L=0.42. The wing shocks were somewhat stronger at this condition as shown in figure 11. CDISC was able to reduce the upper surface shock strengths within the confines of the flow and geometry constraints and achieved a drag reduction of just over 12 counts. While it is probably possible to achieve a greater drag reduction at this specific design condition, the optimum rooftop constraint was purposely formulated to generate target pressures that would also have good off-design performance. The weak shock on the lower surface at the inboard station (figure 11a) was increased slightly in strength, and though the increase in wave drag was insignificant, it could be of concern relative to separation and would have to eventually be evaluated using a Navier-Stokes calculation.

Having obtained satisfactory designs at each of the cruise design points, the WAG multipoint design method was then applied. A mission was arbitrarily assumed that would assign equal weightings to the drag at each design point. For this exercise, the WAG method was modified slightly. Instead of simply using the total drag for each configuration at each design condition to determine the geometry weighting factors, the section drag at each spanwise design station was used. This allowed a spanwise variation in weighting factor and thus greater flexibility in reducing the combined drag objective function. Two approaches to computing the section drag were tried: simple pressure integration and a wave drag estimation technique similar to the one described in reference 16. The latter approach produced results that were more consistent with trends based on total drag values from USM3D, so it was selected for this study.

The two design geometries were run at the opposite design conditions and, by using the restart files from the designs at those conditions, required only 150 flow solver iterations to reach convergence. The design and analysis results were then fed into the WAG module, which computed the wave drag values and determined geometry weighting factors at each of the ten design stations on the wing. The weighting factors varied, but in general tended to use more of the M=0.78 design airfoils. The new geometry was analyzed at both design conditions and the resulting drag coefficients are plotted in figure 12, along with values for the baseline and the point designs. The multipoint design shows a consistent drag reduction relative to the baseline at both design points. The combined drag objective functions for the baseline, M=0.75 design, M=0.78 design, and multipoint design are 0.0236, 0.0232, 0.0229, and 0.0228, respectively. It can be seen that, in spite of the poor off-design performance of the M=0.75 configuration, all of the designs had better multipoint performance than the baseline. The M=0.78 design had performance very similar to the multipoint design as might be expected from the weighting factors.

The pressure distributions for the three designs at the two design conditions are shown in figure 13 and 14. At the lower design Mach number (figure 13), both the M=0.78 and multipoint designs have a mild double shock pattern, but the primary shock for the multipoint design is weaker at each station. At the higher design Mach number (figure 14), the multipoint design has slightly stronger shocks than the M=0.78 design, but they are considerably weaker than the shocks for the M=0.75 design, which had higher drag than the baseline at this condition.

A second cycle through the WAG method produced slightly different weighting factors, but did not improve the objective function. This approach that allows spanwise variation of the weighting factors is still under development, but in this case it seemed to produce a good multipoint design at the additional cost of about 2 full analysis runs after the 2 point designs were obtained.

Canopy design

With a reasonable wing design in hand, attention was then turned to the other regions on the aircraft with strong shocks. For all of the design cases that follow, the multipoint design configuration, run at the primary (M=0.75) design point, served as the baseline. Referring back to figure 8, a strong shock can be seen just aft of the canopy along the crown of the fuselage. To reduce the strength of this shock, a single flow constraint that limits the local Mach number to 1.1 was imposed. In the absence of any other constraints, this would have been an easy goal to achieve. In order to make the exercise more realistic, the following constraints were arbitrarily imposed: first, the nose geometry was fixed, assuming that it houses avionic equipment; second, an internal hard surface constraint was defined to simulate a cockpit space requirement; and finally, the aft end of the design region was fixed just beyond the canopy to minimize the impact on the constant fuselage cross-sections that follow. Additional smoothing of the design region beyond what is normally done in CDISC was included to ensure a smooth transition into the fixed portions of the fuselage.

Mach number contours for a view looking down on the canopy area are shown in figure 15, with the right half of the fuselage representing the baseline flow and the left half showing the results after 20 design cycles. The contours highlighted as dark lines begin at M=1.20 and increase in increments of 0.1. It can be seen that the design has reduced the extent and magnitude of the flow acceleration over the canopy, pulling the maximum Mach number below 1.3, which should help prevent separation. Pressure coefficients along the crown line are shown in figure 16, with the actual design region extending from x/c=0.15 to x/c=0.60 on the plot. The peak Mach number ahead of the shock near the middle of the design region has been reduced significantly, but could not achieve the target pressures because of the geometry constraints. In particular, the cockpit space constraint, shown by the dash-dot line, can be seen to be active. In spite of these limitations, the new design reduced the drag of the configuration by about 28 counts, with no significant change to the lift and pitching moment. While this is considerably greater than the drag reduction obtained on the wing, it is likely that a baseline configuration in a real design exercise would have better performance and the improvement through design would be less. The reduction in shock strength, along with the softened compression region near the beginning of the windshield, should have a favorable impact on the any flow separation occurring in this area.

Aft-fuselage design

The final design exercise in this study addressed the shocks in the aft-fuselage/pylon/nacelle area. A close-up view of the Mach contours in this area (figure 17) reveals strong shocks on the fuselage near the trailing-edge of the wing where the afterbody closure begins. This includes a shock in the channel between the fuselage, pylon, and nacelle, where local Mach numbers exceed the separation criteria of M=1.3. This design focused on the channel region and was done in two stages in order to assess what component, if any, had a dominant influence on the flow expansion and shock. The first stage involved a local redesign of the fuselage with a flow constraint limiting the local Mach number to less than 1.1, as was done for the canopy design. For this case, however there was no hard surface constraint, so that the fuselage could change as much as required. This design was somewhat slower to converge than the wing design cases, requiring 25 design cycles and taking about the same amount of time as the original analysis-only run. A second design was then done, using similar constraints on the inboard side of the nacelle, while allowing the fuselage design to continue to adjust to the changing channel flow. For both of these designs, the pylon airfoil sections and chord lengths were kept fixed, but the planform could change based on the new spanwise locations of the pylon/fuselage and pylon/nacelle intersections.

The Mach contours for the final design case are shown in figure 18. The local Mach numbers on the fuselage just under the pylon and on the pylon itself have been reduced well below the separation criteria. Even though the design region did not extend down into the high-Mach contours just above the wing trailing edge, the flow in this area also benefited from the fuselage modifications made above it. Figure 19 shows the baseline and final design pressure distributions and geometries along a waterline on the fuselage just below the pylon. The strong shock was essentially eliminated, but this required a fairly large geometry change. Obviously, constraints on internal volume or surface curvature may prevent such a modification, and the multipoint performance would have to be evaluated, but CDISC was able to reduce the drag by 17 counts in this case.

For a station on the nacelle just below the pylon (figure 20), the shock near x/c = 0.4 was reduced, but the leading-edge peak was strengthened enough to cause a shock to form ahead of the beginning of the design region (x/c=0.16). This would explain why the second design achieved very little additional drag reduction beyond the 17 counts obtained with just the fuselage design. Being able to design all the way to the leading edge would probably provide the opportunity for

additional performance improvements, but constraints on leading-edge radius and internal hardware would have to be included. It should also be noted that the nacelle design was limited to the inboard side near the pylon, and that the issue of nacelle symmetry would have to be addressed.

Although the pylon was not designed in this exercise, the pressure distribution and geometry at a station about midway between the fuselage and nacelle is shown in figure 21. The strong shock on the lower surface and the moderate shock on the upper surface have both been weakened as a result of the design of the channel between the fuselage and nacelle. The mismatch in shock strengths would indicate that some additional drag reduction could be achieved by recambering the pylon.

The performance of the multipoint-wing, canopy and aft-fuselage/nacelle designs relative to the baseline configuration is shown in figure 22 for both design conditions. The cumulative result of these designs at the primary (M=0.75) design point was a reduction in the inviscid drag of more than 53 counts, or about 23 percent, relative to the baseline. An even larger benefit of about 61 drag counts was obained at the second design point, even though the wing was the only component designed at both conditions. As stated earlier, these are probably larger improvements than might normally be expected when starting from a more refined baseline. The effects of viscosity, in particular flow separation, would also still have to be evaluated using Navier-Stokes analysis, but all of the design changes that were made would be expected to have a beneficial effect on the viscous drag component as well.

Concluding Remarks

As aerospace and other industries push for an edge in an increasingly competitive global market, the role of CFD in the aerodynamic design process will continue to increase. The desire to model the flow about more complete configurations at a variety of flow conditions will continue to push the state-of-the-art toward viscous analysis on large grids. The examples in this paper have shown that, with the CDISC and WAG design methods, it is possible to do constrained multipoint design on a configuration using the same large grids as used for analysis, and to do so with run times that are essentially the same as an analysis-only run. The modular approach to CDISC has allowed it to be coupled with a variety of flow solvers and gridding approaches, and thus provides the option of choosing an analysis method that is already part of a company's inventory and that can most easily meet the modeling requirements.

As a final note, while CDISC cannot replace optimization in cases where the relationships between geometry changes, flow physics and improved performance are not understood, it appears to be a very efficient and effective approach when they are understood. It would seem that the roles of the two approaches are therefore complementary, with optimization helping to build a knowledge base that could be efficiently applied by a method like CDISC. As work continues to make both approaches more efficient, effective and user-friendly, the goal of viscous design of full configurations, even at high-lift conditions with all surfaces deployed, will become a reality.

Acknowledgments

The author would like to thank Dr. Paresh Parikh of Paragon Research Associates, Inc. and Javier Garriz of ViGYAN, Inc. for supplying the grids, other files, and advice needed for running the generic business jet case in the unstructured grid flow solver.

References

[1]Jameson, Antony: Re-Engineering the Design Process through Computation. AIAA-97-0641, 1997.

[2]Jou, W.H.; Huffman, W.P.; Young, D.P.; Melvin, R.G.; Bieterman, M.B.; Hilmes, C.L.; and Johnson, F.T.: Practical Considerations in Aerodynamic Design Optimization. AIAA-95-1730-CP, 1995.

[3]Cao, H.V.; and Blom, G.A.: Navier-Stokes/Genetic Optimization of Multi-Element Airfoils. AIAA-96-2487, 1996.

[4]Foster, Norman F.; and Dulikravich, George S.: Three-Dimensional Optimization Using Genetic Evolution and Gradient Search Algorithms. AIAA-96-0555, 1996.

[5]Ogot, Madara; Aly, Sherif; Pelz, Richard B.; Marconi, Frank; and Siclari, Michael: Stochastic Versus Gradient-based Optimizers for CFD Design. AIAA-96-0332, 1996.

[6]Hicks, R.: Wing Design by Numerical Optimization. AIAA-77-1247, 1977.

[7]Chang, I-Chung; Torres, Francisco J.; and van Dam, C. P.: Wing Design Code Using Three-Dimensional Euler Equations and Optimization. AIAA-91-3190, 1991.

[8]Reuther, J.; Cliff, S.; Hicks, R.; and van Dam, C.P.: Practical design optimization of wing/body configurations using the Euler equations. AIAA-92-2633, 1992.

[9]Huffman, W.P.; Melvin, R.G.; Young, D.P.; Johnson, F.T.; Bussoletti, J.E.; Bieterman, M.B.; and Hilmes, Craig L.: Practical Design and Optimization in Computational Fluid Dynamics. AIAA-93-3111, 1993.

[10]Burgreen, Greg W.; and Baysal, Oktay: Three-Dimensional Aerodynamic Shape Optimization of Wings Using Sensitivity Analysis. AIAA-94-0094, 1994.

[11]Hou, G.J.-W.; Maroju, V.; Taylor, A.C.; Korivi, V.M.; and Newman, P.A.: Transonic Turbulent Airfoil Design Optimization with Automatic Differentiation in Incremental Iterative Forms. AIAA-95-1692, 1995.

[12]Reuther, J.; Alonzo, J.J.; Vassberg, J.C.; Jameson, A.; and Martinelli, L.: An Efficient Multiblock Method for Aerodynamic Analysis and Design on Distributed Memory Systems. AIAA-97-1893, 1997.

[13]Reuther, J.; Jameson, A.; Alonso, J.J.; Rimlinger, M.J.; and Saunders, D.: Constrained Multipoint Aerodynamic Shape Optimization Using an Adjoint Formulation and Parallel Computers. AIAA-97-0103, 1997.

[14]Jameson, A.; Pierce, N.A.; Martinelli, L.: Optimum Aerodynamic Design using the Navier-Stokes Equations. AIAA-97-0101, 1997.

[15]Anderson, W. Kyle; and Venkatakrishnan, V.: Aerodynamic Design Optimization on Unstructured Grids with a Continuous Adjoint Formulation. AIAA-97-0643, 1997.

[16]Campbell, Richard L.: An Approach to Constrained Aerodynamic Design With Application to Airfoils. NASA TP 3260, November, 1992.

[17]Campbell, Richard L.: Efficient Constrained Design Using Navier-Stokes Codes. AIAA-95-1808, 1995.

[18]Naik, D.; Krist, S.; Vatsa, V.; Campbell, R.; Buning, P.; and Gea, L.: Inverse Design of Nacelles Using Multiblock Navier-Stokes Codes. AIAA-95-1820, 1995.

[19]Parikh, Paresh: Development of a Modular Aerodynamic Design System based on Unstructured Grids. AIAA-97-0172, 1997.

[20]Campbell, Richard L.; and Smith, Leigh A.: A Hybrid Algorithm for Transonic Airfoil and Wing Design. AIAA-87-2552-CP, 1987.

[21]Chan, William M.; Rogers, Stuart E.; Nash, Steven, M.; and Buning, Pieter G.: Manual for Chimera Grid Tools, Version 0.5. April, 1998. (Available from authors at NASA Ames Research Center, Moffett Field, CA, 94035)

[22]Vatsa, V. N.; Sanetrik, M. D.; and Parlette, E. B.: Development of a Flexible and Efficient Multigrid-Based Multiblock Flow Solver. AIAA-93-0677, 1993.

[23]Thomas, J.L.; Taylor, S.L.; and Anderson, W.K.: Navier-Stokes Computations of Vortical Flows Over Low Aspect Ratio Wings. AIAA-87-0207, 1987.

[24]Abdol-Hamid, K.S.: Application of a Multiblock/ Multizone Code (PAB3D) for the Three-Dimensional Navier-Stokes Equations. AIAA-91-2155, 1991.

[25]Swanson, R.C.; and Turkel, E.: Multistage Schemes With Multigrid for Euler and Navier-Stokes Equations - Components and Analysis. NASA TP 3631, August, 1997.

[26]Buning, P. G.; Parks, S. J.; Chan, W. M.; and Renze, K. J.: Application of the Chimera Overlapped Grid Scheme to Simulation of Space Shuttle Ascent Flows. Presented at the 4th International Symposium on Computational Fluid Dynamics, Davis, CA, September 9 - 12, 1991.

[27]Frink, N. T.: Assessment of an Unstructured-Grid Method for Predicting 3-D Turbulent Viscous Flows. AIAA-96-0292, 1996.

[28]Frink, Neal T.; Pirzadeh, Shahyar; and Parikh, Paresh: An Unstructured-Grid Software System for Solving Complex Aerodynamic Problems. NASA CP-3291, May, 1995.

[29]Anderson, W.K.; and Bonhaus, D.L.: An Implicit Upwind Algorithm for Computing Turbulent Flows on Unstructured Grids. Computers and Fluids, Vol. 23, No. 1, 1994, pp. 1-21.

[30]Lovell, D.A.; and Doherty, J.J.: Aerodynamic Design of Aerofoils and Wings Using a Constrained Optimisation Method, ICAS-94-2.1.2, 1994.

[31]Pirzadeh, S.: Progress Toward a User-Oriented Unstructured Viscous Grid Generator, AIAA-96-0031, 1996.

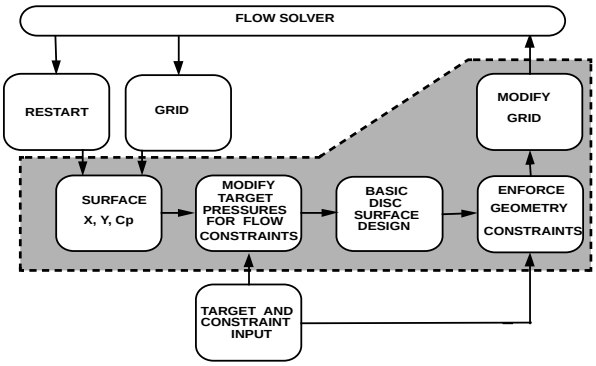

Figure 1. Flow chart of the CDISC design system.

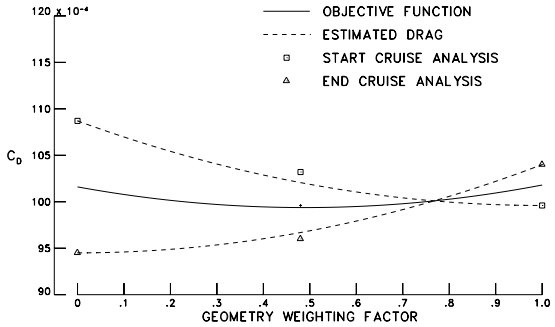

Figure 4. Airfoil design results using the WAG method.

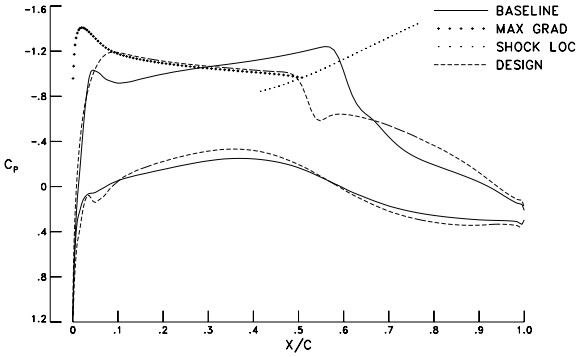

Figure 2. Illustration of the optimum transonic rooftop flow constraint.

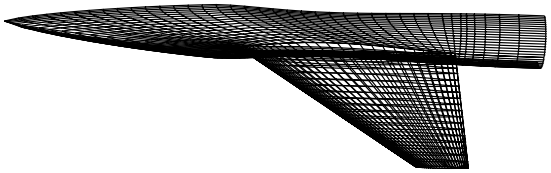

Figure 5. Generic fighter surface grid.

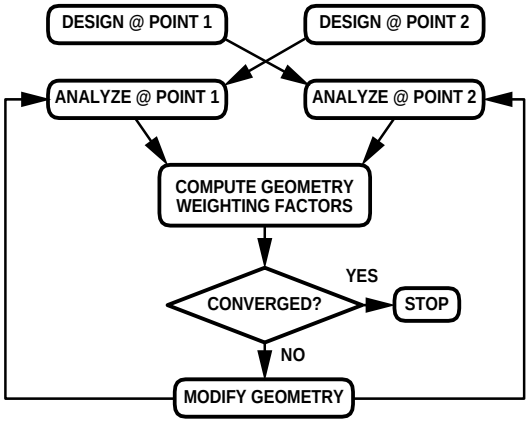

Figure 3. Flow chart of the WAG multipoint design method.

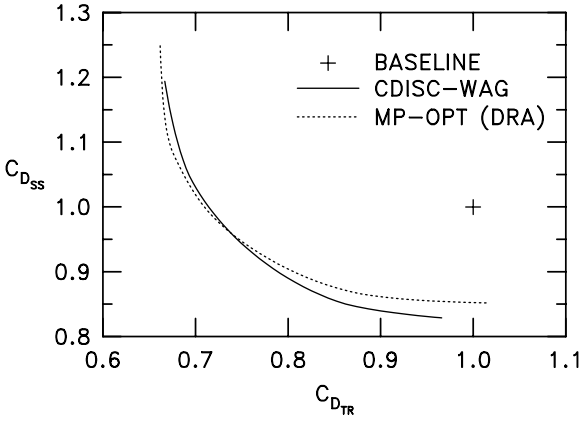

Figure 6. Comparison of WAG and optimization results for multipoint design of a generic fighter.

Figure 7. Unstructured surface grid for a generic business jet.

Figure 8. Mach contours for a generic business jet at M=0.75, C_L=0.48.

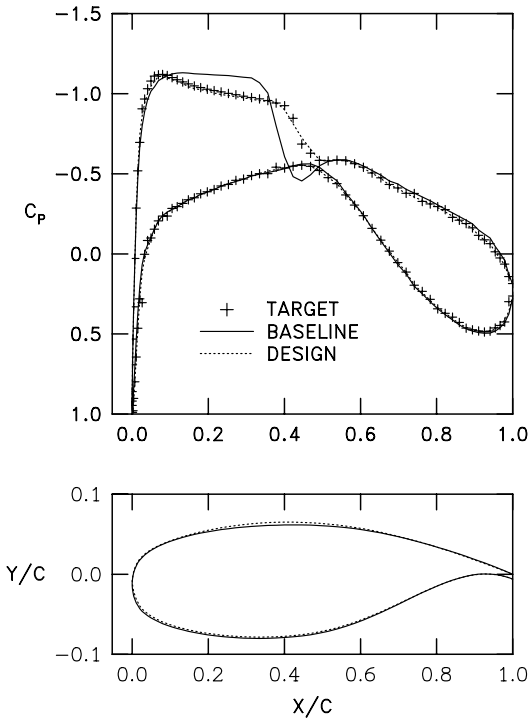

a) η=0.4

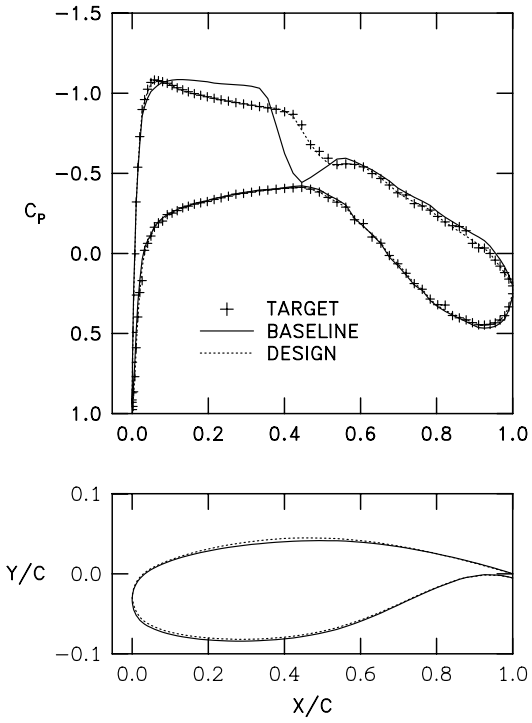

b) η=0.8

Figure 9. Wing design results at M=0.75, C_L=0.48.

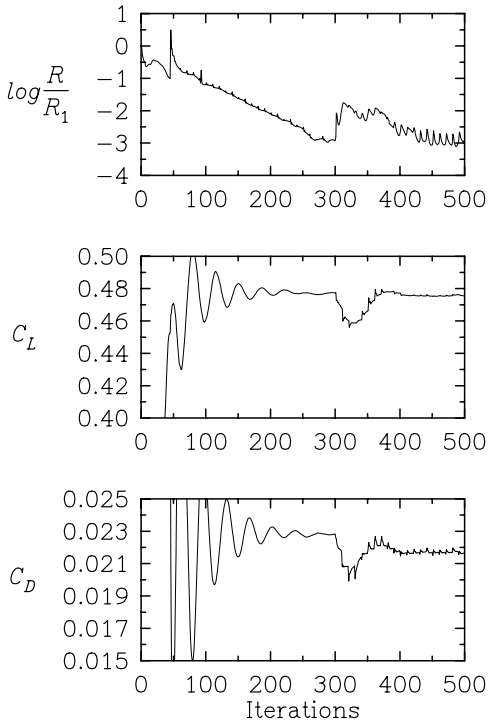

Figure 10. USM3D convergence history for baseline analysis and wing design at M=0.75, C_L=0.48.

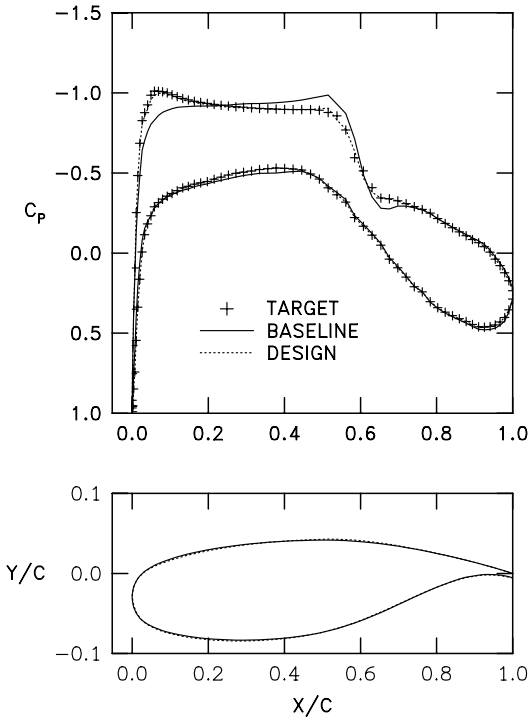

b) η=0.8

Figure 11. Concluded.

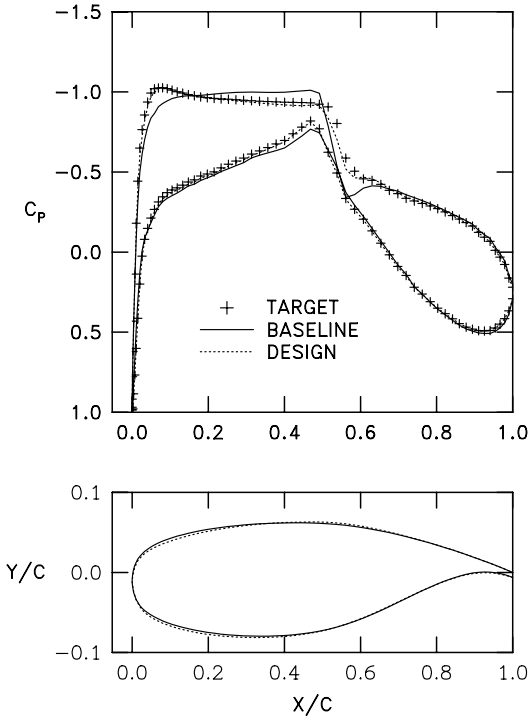

a) η=0.4

Figure 11. Wing Design results at M=0.78, C_L=0.42.

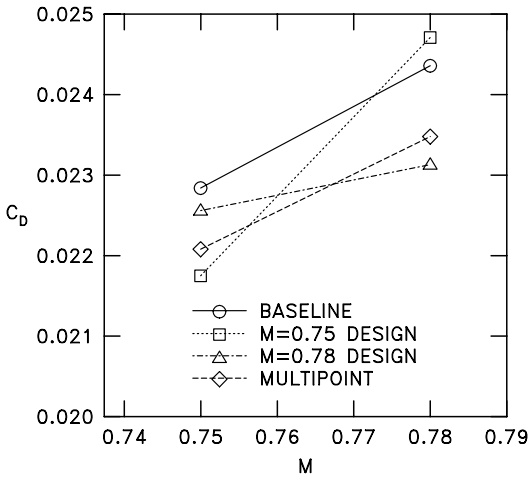

Figure 12. Comparison of drag coefficients for the baseline, single-point, and multipoint designs.

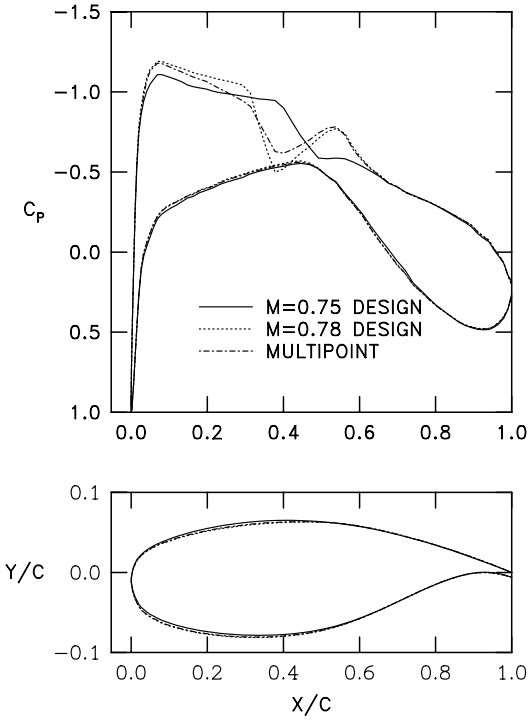

a) η=0.4

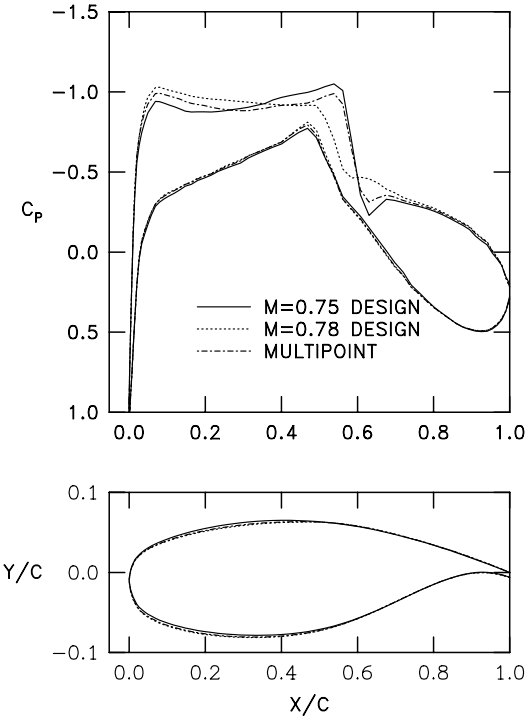

a) η=0.4

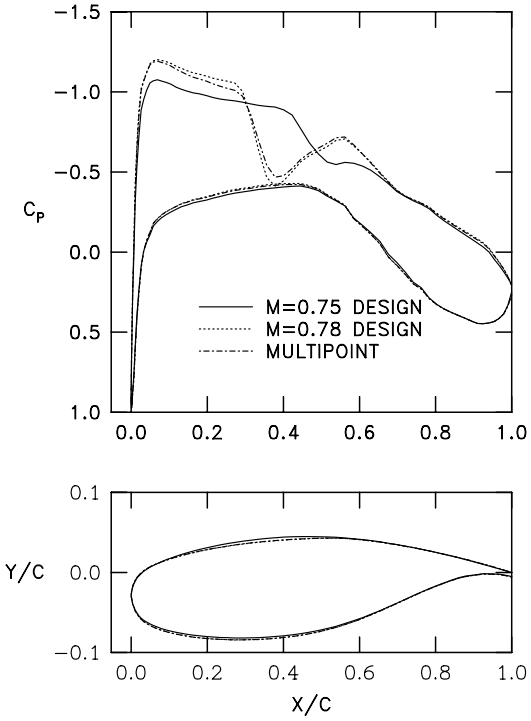

b) η=0.8

Figure 13. Comparison of single-point and mutlipoint design results at M=0.75, C_L=0.48.

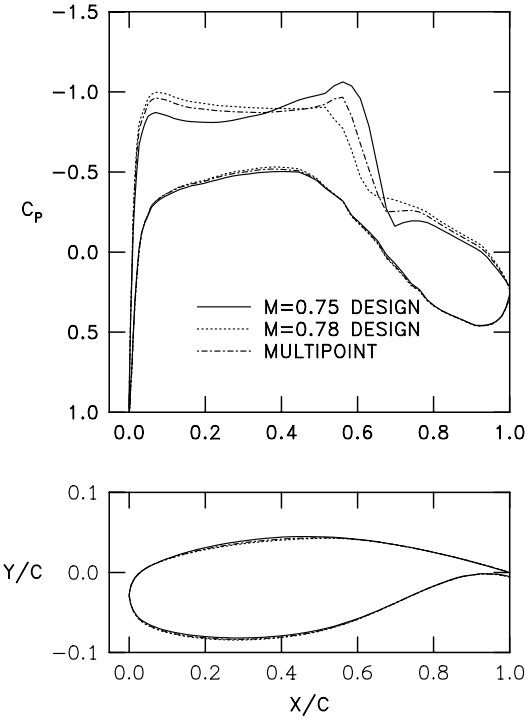

b) η=0.8

Figure 14. Comparison of single-point and multipoint design results at M=0.78, CL=0.42.

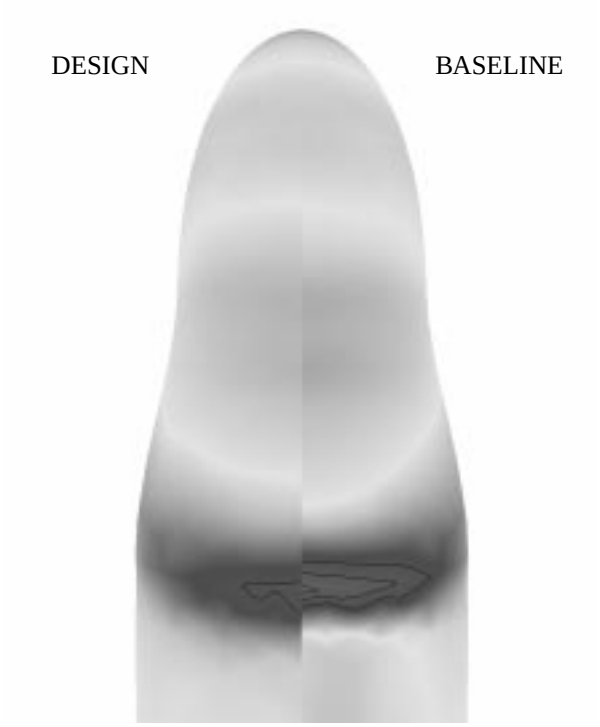

Figure 15. Mach contours in the canopy region for the baseline and design at M=0.75, C_L=0.48.

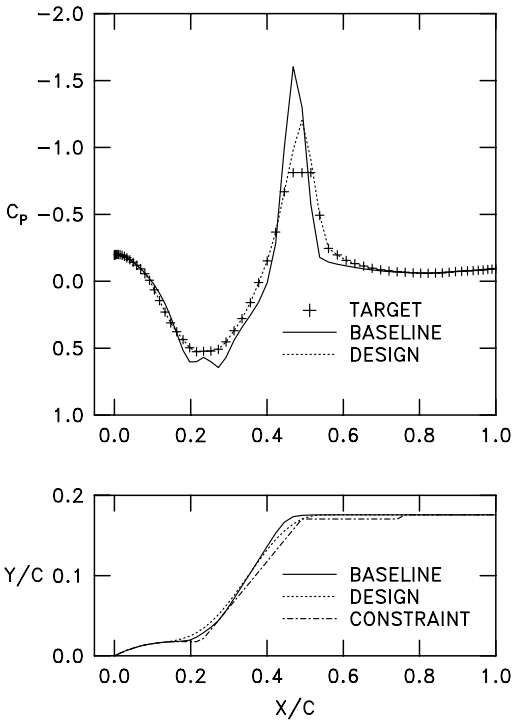

Figure 16. Design results along the crown line in the canopy region at M=0.75, C_L=0.48.

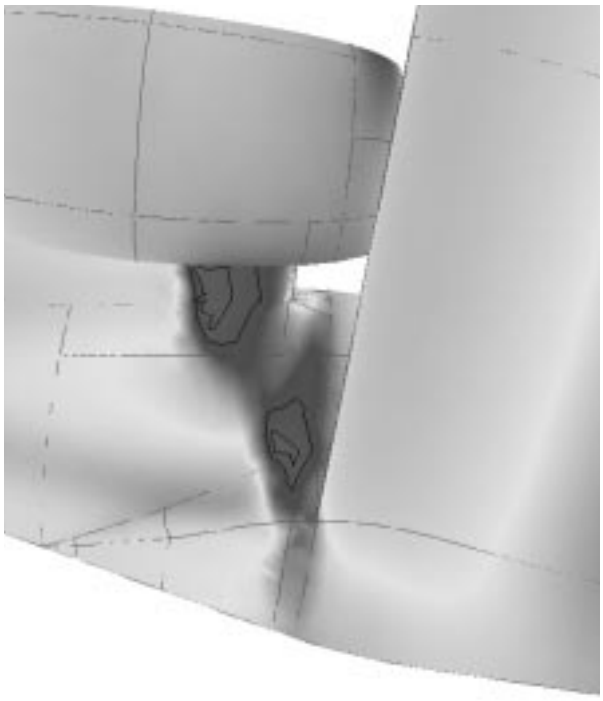

Figure 17. Mach contours in the aft-fuselage region for the baseline at M=0.75, C_L=0.48.

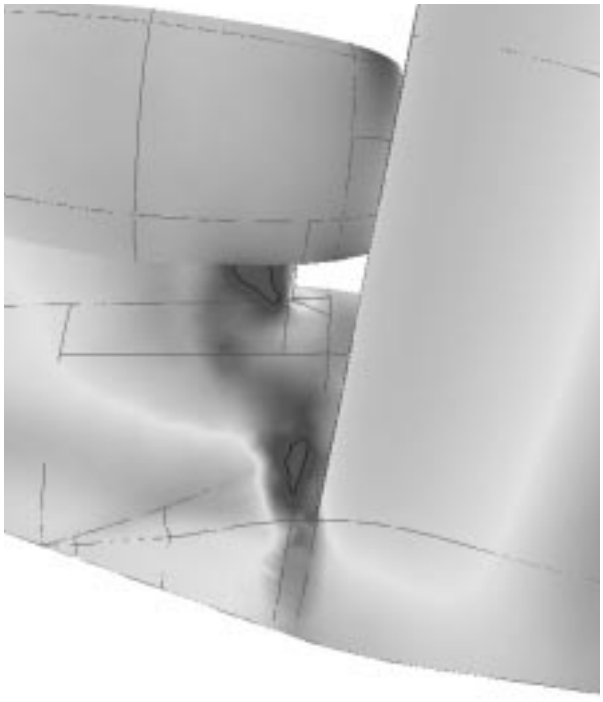

Figure 18. Mach contours in the aft-fuselage region for the final design at M=0.75, C_L=0.48.

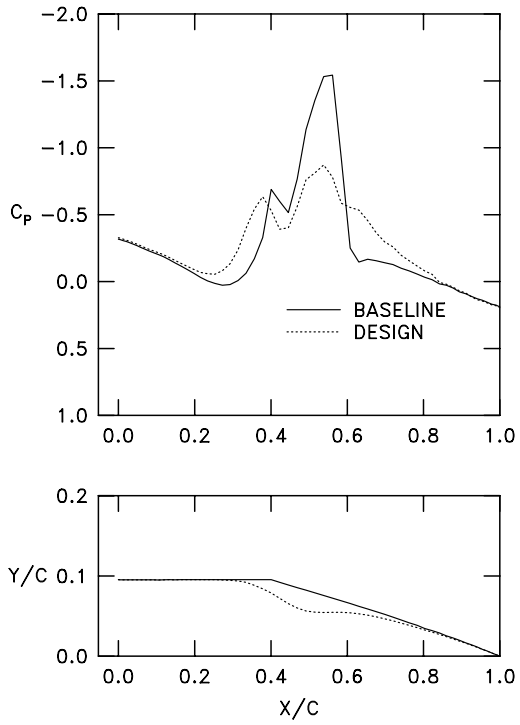

Figure 19. Design results along a waterline on the fuselage just below the pylon at M=0.75, C_L=0.48.

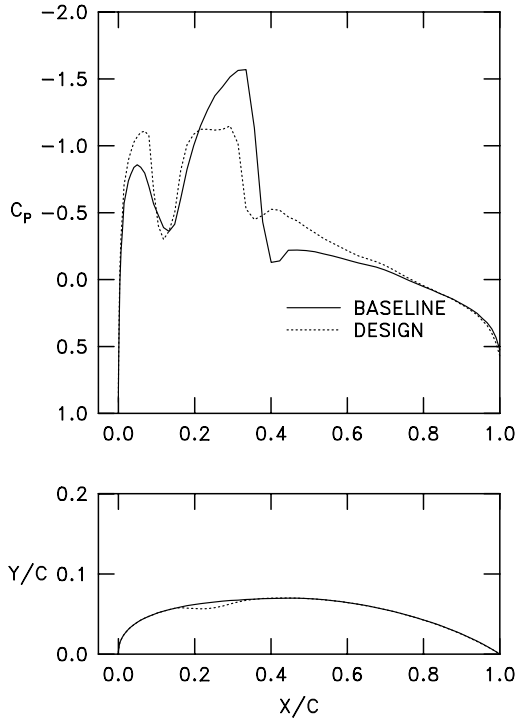

Figure 20. Design results along a waterline on the nacelle just below the pylon at M=0.75, C_L=0.48.

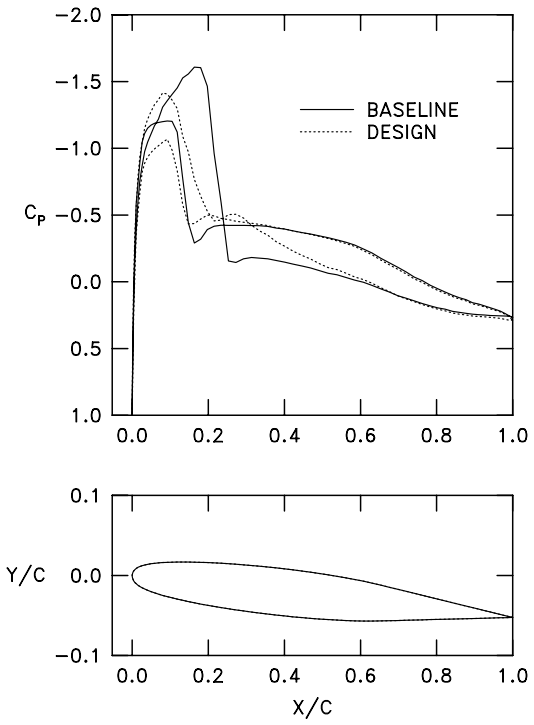

Figure 21. Effect of fuselage and nacelle design at a station near midspan on the pylon at M=0.75, C_L=0.48.

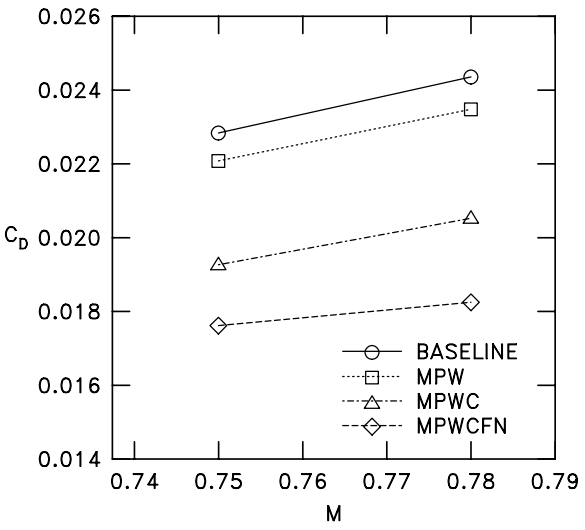

Figure 22. Performance of the multipoint wing, canopy, and aft-fuselage/nacelle designs relative to the baseline.